

CALORIMETRIC AND IONIZATION MEASUREMENTS OF
STOPPING POWER IN CARBON FOR 19.5 GeV ELECTRONS*

Kenneth R. Kase† and Steve R. Domen††
Stanford Linear Accelerator Center
Stanford University, Stanford, Calif. 94305

ABSTRACT

A portable carbon calorimeter built at the National Bureau of Standards was used in a 19.5 GeV electron beam at the Stanford Linear Accelerator to measure absorbed dose. The dose measurements were normalized to a given number of incident electrons by monitoring the electron intensity with a transmission ion chamber previously calibrated against a quantameter in the same beam. The simultaneous measurement of integrated electron intensity and absorbed dose allowed a direct determination of stopping power in carbon for 19.5 GeV electrons. The measured value of $1.80 \text{ MeV} \cdot \text{cm}^2 \cdot \text{g}^{-1}$ is within 6% of the calculated value.

(Submitted to Nucl. Instr. and Meth.)

* This work was performed under the auspices of the U.S. Atomic Energy Commission.

† Department of Radiology, Stanford University, Stanford, Calif. 94305.

†† Center for Radiation Research, NBS, Washington, D.C. 20234.

I. Introduction

Some new calorimetric methods having general application have been devised^{1,2} and applied to an absorbed-dose calorimeter at the National Bureau of Standards (NBS). One feature of this calorimeter is that it is small and can be transported relatively easily. This report describes its first use as a field instrument. It also describes the first calorimetric absorbed dose measurements made in a high-energy (19.5 GeV) electron beam at the Stanford Linear Accelerator Center (SLAC). The calorimeter was constructed as part of an NBS program to measure absorbed dose for electron and photon beams of energies up to 50 MeV, but this report indicates that there is no apparent upper limit to the beam energy for which a calorimeter can be used.

The use of this calorimeter at SLAC introduced less favorable conditions than those ordinarily encountered. The ambient temperature fluctuations were large, the dose rate was small and the electron beam was smaller in cross section than the calorimetric absorber.

Since the number of incident electrons was monitored during the absorbed dose measurements, an interesting result was a direct determination of the mean energy deposition per electron in a carbon absorber of known dimensions. The measured energy loss is found to agree with a calculation of energy loss to within six percent.

II. Calorimeter Description

The calorimeter is designed to decrease effects of four types of thermal gradients, and to permit rapid measurements.* Figure 1 shows a side view cross section of the assembled carbon (graphite) components. Figure 2 is a

* A detailed description of the calorimeter and its operation is in manuscript.

disassembled view of its internal structure, the core, jacket, and shield. This thermally floating assembly is mounted in a hole of a temperature-regulated medium (fig. 3). The calorimetric core is 2 cm in diameter and 2.8 mm (452 mg/cm^2) thick, and its heat capacity is equal to that of the jacket. Temperature responses are observed in the core during beam irradiation, and they are automatically summed in the core and jacket during electrical calibration. The narrow beam first passes through the mylar and carbon windows, and then through the shield and jacket caps, which is a total thickness of 638 mg/cm^2 .

The calorimeter, its measurement and control circuits, amplifier, vacuum gauge and 35-meter cable lengths were easily transported. A strip chart recorder, digital voltmeter, decade resistor and vacuum pumping equipment were supplied by SLAC.

Speed of measurement depends upon how rapidly the calorimeter can be restored sufficiently near its initial equilibrium condition after a heating run. This is the usual method of operation and the degree to which this can be attained depends on the power to be measured. The time usually required is several minutes when measuring calibration runs or high dose rate runs. The time increases as lower dose rates are to be measured. The bodies can be brought from room temperature to their separate equilibrium temperatures near 30°C in less than two hours.

III. Experimental Setup

The electron beam used for the calorimetric measurements was a primary beam from the SLAC accelerator. The beam was attenuated in a two-stage scatterer and collimator system and momentum analyzed to $\pm 1\%$. The attenuation was such that a maximum beam intensity of 10^6 electrons per pulse was attainable with a peak beam current of 10 mA. The beam cross section could

be varied within limits by adjusting the focussing. The dose measurements were done using a beam which measured $7 \text{ mm} \times 7 \text{ mm}$ on a film placed at the calorimeter position. The pulse repetition rate during the measurements was either 10 per second or 60 per second. The electron energy was 19.5 GeV.

A diagram of the experimental setup is shown in fig. 4. The calorimeter was aligned in the beam photographically by placing a wire cross hair on the central axis of the core on both the upstream and downstream faces of the calorimeter. A film was placed downstream of each cross hair and exposed with the beam (fig. 5).

The beam intensity was continuously monitored with a transmission ion chamber which was calibrated against a quantameter³ in the same beam⁴. By integrating the charge collected in the ion chamber during the period of a calorimeter run, we were able to determine the number of electrons which passed through the calorimeter during the absorbed dose measurements. The ion chamber charge integration was done with a high gain, feedback electrometer. Alignment of the ion chamber in the beam was also done photographically.

IV. Absorbed Dose Measurements

Figure 6 is a photograph of the temperature sensor output strip chart recording during a run where time increases from right to left. The net temperature rise is an absolute measure of the absorbed dose averaged over the 2 cm diameter graphite core. Occasionally, noise signal pulses were observed which were attributed to external sources. It was found necessary to observe the initial drift rate with a 1 pulse/s beam to assure favorable irradiation conditions when a 10 or a 60 pulse/s rate was started. The net dose rate averaged 0.18 rad/s and ranged from 0.1 to 0.3 rad/s. Irradiation times varied from 10 to 23 minutes. Soon after beam turn-off the 1 pulse/s drift

was continued, and both curves were extrapolated to the mid-run where the bridge null resistance was determined.* The estimated uncertainties of the experimental determinations are listed in the last column of table 1 and are generally less than 2%. The net measured dose from a 9 or 59 pulse/s exposure was compared to the net number of measured incident electrons, N_e . The relative standard deviation of the mean is 1.3%.

These measurements differed from those made under laboratory test conditions. Since the background drifts were partly formed by a fraction of the beam intensity, intensity variations affected the extrapolated values at the midrun. This contributed to the spread of the results. The duration of the runs, from the beginning of the initial drift to the termination of the final drift, varied from 1/2 hour to 1 hour. Changes in beam intensity were observed, but were not continuously recorded. Several times sizable changes were noted and corrections were applied. The narrowness of the beam increased the heat loss corrections since the beam did not heat the entire jacket and shield. The room temperature varied between 16° and 26°C and five of the measurements were made when the temperature was changing at a rate about 1°C/hour. The influence this had on the measurements is uncertain, but a laboratory test showed that a change in room temperature will produce a change in drift during the runs. Nevertheless, considering the spread of the results, the performance of the calorimeter is considered to be satisfactory.

*Theoretical calculations, which assumed a constant beam intensity and background drift, verified the accuracy of the extrapolations. Approximately known irradiation and calorimetric parameters were substituted into a three-body solution, which resulted in heat loss corrections ranging from 7 to 17%. The extrapolated values predicted by parabolic fits to the final cooling curves agreed within 0.2% with theoretical values derived by assuming no heat loss from the core.

The calorimeter was tested at NBS in a large diameter and constant intensity beam of $^{60}\text{Co}\gamma$ rays. The dose rate and exposure times were comparable to those at SLAC, 0.12 rad/s applied from 15 to 24 minutes. The room temperature variation at NBS was 0.3°C/day . Measurements of the dose rate showed that the standard deviation of the mean was about 1/2%. The measured dose rate at NBS agreed within 1% with that measured with an ionization chamber of known volume having dimensions similar to the calorimeter core.

V. Results

Of the nine calorimeter runs made in the 19.5 GeV electron beam, only seven were used in the calculation of absorbed dose per electron. Table 1 shows the results of the seven runs used. Run No. 1 was excluded because the total number of electrons was not measured. Run No. 7 was excluded because it is uncertain whether the background rate was 1 or 10 pulses per second. During the two runs at 60 pulses/s the beam current was intentionally lowered to check the recombination correction in the ion chamber. For each run the absorbed dose was measured, the charge collected by the ion chamber was integrated and the exposure time measured. A first estimate of the total number of electrons, N_e , was made from the integrating charge. This was then used with the exposure time to calculate the average number of electrons per second. Knowing the pulse rate, a recombination correction⁴ for the ion chamber could then be made to determine a better value of N_e . This correction ranged from 2 to 7%. The rather large estimated uncertainty in the determination of N_e is caused by the uncertainty in the calibration of the monitor ion chamber. The percent standard deviation of the mean for 53 calibration points was 6.6%.

From the data tabulated in Table 1 a weighted average dose per electron was calculated. Each run was weighted by the inverse of the estimated uncertainty for that run. The weighted average is $D/N_e = 9.19 \times 10^{-9}$ rad/electron. The

relative standard deviation of the mean for the seven runs is 1.3% while the estimated maximum uncertainty in the measurements is 8%.

From the measurement of D/N_e and from the cross sectional area of the calorimeter core we can calculate the average energy per unit path length deposited in the core, $1.80 \text{ MeV-cm}^2 \text{-g}^{-1}$ per electron.

VI. Comparison with Theory

The energy deposited in the calorimeter core by 19.5 GeV electrons can be calculated by a consideration of energy loss mechanisms. These electrons lose about 98% of their energy by generating bremsstrahlung, which escapes the core without further interaction. A calculation indicates that less than 0.1% of the total energy deposition in the core is due to bremsstrahlung. Consequently this mechanism is the local absorption of energy from low energy secondary electrons generated in the core and in the calorimeter components upstream from the core. This energy was calculated in three steps.

First, consider the energy transferred to secondaries which are generated in the core but which do not have enough energy to escape from the core. It can be calculated with the help of the formula for "restricted stopping power" for electrons as given by Berger and Seltzer⁵:

$$L_{\Delta} = \frac{2 \pi N_a r_0^2 mc^2}{\beta^2} \frac{Z}{A} \left\{ \ln \left[\frac{2(\tau + 2)}{(I/mc^2)^2} \right] - 1 - \beta^2 + \ln [(\tau - \Delta)\Delta] + \tau/(\tau - \Delta) + \left[\Delta^2/2 + (2\tau + 1) \ln(1 - \Delta/\tau) \right] / (\tau + 1)^2 - \delta \right\}, \quad (1)$$

where:

N_a = Avogadro's number,

r_0 = e^2/mc^2 ,

e = electron charge,

- m = electron mass,
 c = velocity of light,
 β = electron velocity, in units of c ,
 Z = atomic number of medium,
 A = mass number of medium,
 τ = T/mc^2
 T = electron kinetic energy,
 I = mean excitation energy of medium,
 Δ = T'_c/mc^2 ,
 T'_c = cutoff kinetic energy,
 δ = density effect correction.

The quantity L_{Δ} represents the energy per unit path length transferred from a primary electron of energy T to secondary electrons with energies no larger than T'_c . Physically T'_c specifies a limiting energy transfer to secondary electrons. It is assumed that any secondary which receives an energy T'_c or less in a collision deposits all its energy in the core, while any secondary which receives an energy greater than T'_c in a collision in the core escapes the core and deposits no energy. * T'_c is a function of depth in the core, and the functional relationship can be determined from a comparison of collision geometry (fig. 7) with the kinematics of electron-electron collisions⁶:

$$T' = 2mc^2 \frac{p^2 c^2 \cos^2 \theta}{[mc^2 + (p^2 c^2 + m^2 c^4)^{\frac{1}{2}}]^2 - p^2 c^2 \cos^2 \theta} \approx \frac{2mc^2 \cos^2 \theta}{1 - \cos^2 \theta}, \quad (2)$$

* The cylindrical surface of the core is too far from the edge of the beam for any of the secondaries to escape out the sides.

where:

T' = kinetic energy of secondary electron,

p = momentum of primary electron,

θ = generation of angle of secondary electron.

The second equality in equation (2) follows because $T \gg mc^2$ (so that $pc \gg mc^2$).

Let $T' = T'_c$ in equation (2), and in fig. 7, let $t(T', x) = R[T'_c(x)]$, the range of an electron with energy T'_c . Then, solving (2) for $\cos \theta$ and comparing with fig. 7:

$$\cos \theta = \sqrt{\frac{T'_c}{T'_c + 2mc^2}} = \frac{X-x}{R[T'_c(x)]} \quad (3)$$

Equation (3) can be used to calculate T'_c as a function of x , with the help of range tables⁵. The energy deposited in the core by secondary electrons with energies T'_c or less is then found by integrating equation (1) over position:

$$\epsilon_{\Delta} = \int_0^X L_{\Delta}(x) dx. \quad (4)$$

This integral was evaluated numerically, * using $X = 452 \text{ mg/cm}^2$, and the result is $\epsilon_{\Delta} = 0.718 \text{ MeV/electron}$.

The second step in calculating energy deposited in the core is to account for energy deposited by secondaries generated in the core with energies larger than T'_c , so that they escape from the core. This can be estimated from the equation:

$$\epsilon_e = \int_0^X \int_{T'_c(x)}^{T'_{\max}} \Phi(T, T') \frac{dT'}{dt}(T') t(T', x) dT' dx, \quad (5)$$

* The maximum value of T'_c in this integration was 1.1 MeV.

where:

$$\begin{aligned} \Phi(T, T')dT' &= \text{Moller cross section for electron-electron collisions,} \\ \frac{dT'}{dt}(T') &= \text{mass stopping power for electrons with kinetic energy } T', \\ \text{and } T'_{\text{Max}} &= T/2 = 9.75 \text{ GeV.} \end{aligned}$$

The Moller cross section (ref. 6, p. 15) can be written:

$$\Phi = 2mc^2 \left(\pi N_a \frac{Z}{A} r_0^2 \right) \frac{T^2}{(T-T')^2(T')^2} \left[1 - \frac{T'}{T} + \left(\frac{T'}{T} \right)^2 \right]^2. \quad (6)$$

The integral in equation (5) was evaluated numerically to give $\epsilon_e = 0.021 \text{ MeV/}$ electron.

The third step in calculating energy deposited in the core is to account for energy deposited by secondaries in the calorimeter components just upstream of the core. Figure 8 shows the geometry. The gaps between the window and the core are less than 1 mm and so we assume all escaping secondaries enter the core.

The energy deposited in the core can be calculated from the equation

$$\epsilon_w = \int_0^{X'} \int_{T'_c(x)}^{T'_{\text{max}}} \Phi(T, T') \frac{dT'}{dt}(T') t(T') dT' dx. \quad (7)$$

This equation is very similar to equation (5) except that now $t \leq \frac{X}{\cos \theta}$ and thus a function of T' only, and $X' = 638 \text{ mg/cm}^2$. Also we have $d(T', x) = \frac{X' - x}{\cos \theta}$.

Since some of the secondaries generated in this material will stop in the core, it is necessary to place some restrictions on $\frac{dT'}{dt}(T')$ and $t(T')$ in equation (7). We do this in the following way:

1. If $d(T') + t(T') \geq R(T')$ where as before $R(T')$ is the range of an electron with energy T' , then we define $\tilde{t}(T') = R(T') - d(T')$ and

$\frac{dT'}{dt}(T') = \frac{T'}{R(T')}$ and integrate

$$\epsilon_w = \int_0^{X'} \int_{T'_c(x)}^{T'_{\max}} \Phi(T, T') \frac{T'}{R(T')} \tilde{t}(T') dT' dx.$$

2. In all other cases we integrate equation (7) using tabulated values for

$$\frac{dT'}{dt}(T') \text{ and } t(T') = \frac{X}{\cos \theta}.$$

The result of this integration gives $\epsilon_w = 0.029$ MeV/electron.

It should be pointed out that the change in stopping power along the track of the secondaries has been ignored in the calculations. This will lead to an underestimate of the energy deposition. Energy deposition by secondaries generated in the air path upstream of the calorimeter has been estimated and is negligible. Likewise, the contribution of back-scattering is also negligible.

The total mean energy deposited in the core by a 19.5 GeV electron is then:

$$\bar{\epsilon} = \epsilon_{\Delta} + \epsilon_e + \epsilon_w = 0.768 \text{ MeV/electron.}$$

The calculated average energy deposition per unit path length (stopping power) is $1.70 \text{ MeV cm}^2 \text{ g}^{-1}$ per electron which is smaller than the measured value of 1.80 by 5.5%. This is reasonable agreement considering the uncertainties in the measurements and the calculations.

VII. Summary

A portable calorimeter was used to measure absorbed dose produced by a 19.5 GeV electron beam under conditions which were somewhat severe. The standard deviation of the mean for measurement of the dose per electron is 1.3%. A comparison between measured and calculated stopping power agrees to within 6%.

Acknowledgment

The authors wish to thank those of the SLAC Health Physics Department who participated in the experiment especially W.R. Nelson for his assistance with the numerical integrations. Thanks also are due to M.J. Berger for helpful comments and to J.S. Pruitt for suggesting the method of determining the correction factor ϵ_w . Development of the calorimeter was supported in part by the National Cancer Institute of the National Institutes of Health.

References

1. S.R. Domen, U.S. Patent Number 3,665,762 (May 30, 1972).
2. S.R. Domen, A Heat-Loss-Compensated Calorimeter and Related Theorems, J. Res. (Eng. and Instr.) National Bureau of Standards (U.S.) 73C (Jan-June, 1969) 17.
3. D. Yount, Nucl. Inst. Meth. 52 (1967) 1.
4. K.R. Kase, W.R. Nelson and L. Keller, "Radiation Measurements in Secondary Electron Beams and Comparison with Calculations," Stanford Linear Accelerator Center Report No. SLAC-PUB-1333 (October 1973) (submitted to Health Physics).
5. M.J. Berger and S.M. Seltzer, "Tables of Energy Losses and Ranges of Electrons and Positrons," NASA-SP-3012 (1964).
6. B. Rossi, High-Energy Particles (Prentice-Hall, New Jersey, 1965) p. 14.

Figure Captions

1. Cross section drawing of the assembled portable calorimeter. The core and jacket are equal in heat capacity. Temperature responses in the core are observed during beam irradiation. They are automatically summed in the core and jacket during electrical calibration. The beam passes through 638 mg/cm^2 of carbon before the front core surface.
2. Core-jacket-shield assembly. The jacket cap completes the enclosure of the central core, and the shield cap completes the enclosure of the jacket.
3. Beam exit view of the portable calorimeter showing some details of the outer temperature-controlled carbon medium.
4. Experimental setup. Simultaneous measurements were made of the calorimeter-to-chamber response, and also of the quantameter-to-chamber response, and also of the quantameter-to-chamber response with the calorimeter removed.
5. Alignment of the calorimeter. A $7 \text{ mm} \times 7 \text{ mm}$ beam photographed a lead cross hair placed on the central axis of the calorimetric core.
6. Calorimetric absorbed dose run produced by a 19.5 GeV electron beam, $7 \text{ mm} \times 7 \text{ mm}$.
7. Illustration of the distance travelled, $t(T', x)$, by a secondary electron of energy T' generated at position x in the core of thickness X .
8. Illustration of the geometry for the calculation of the correction factor ϵ_w .

TABLE 1

Ion Chamber and Calorimeter Data

Run No.	N_e (electrons)	Estimated Uncertainty	Recombination Correction	Beam Pulse Rate (sec^{-1})	Net Dose Rate (rad/s)	Absorbed Dose (rad)	Estimated Uncertainty
2	1.44×10^{10}	$\pm 7.5\%$	1.075	10	0.18	130.9	$\pm 1.3\%$
3	1.45×10^{10}	7.5%	1.053	10	0.11	136.0	4.2%
4	1.48×10^{10}	7.5%	1.070	10	0.17	139.8	1.4%
5	1.46×10^{10}	7.5%	1.058	10	0.13	141.3	1.2%
6	1.52×10^{10}	7.5%	1.064	10	0.15	134.4	1.9%
8	1.85×10^{10}	7.5%	1.026	60	0.29	163.5	1.2%
9	2.25×10^{10}	7.5%	1.020	60	0.26	203.9	1.6%

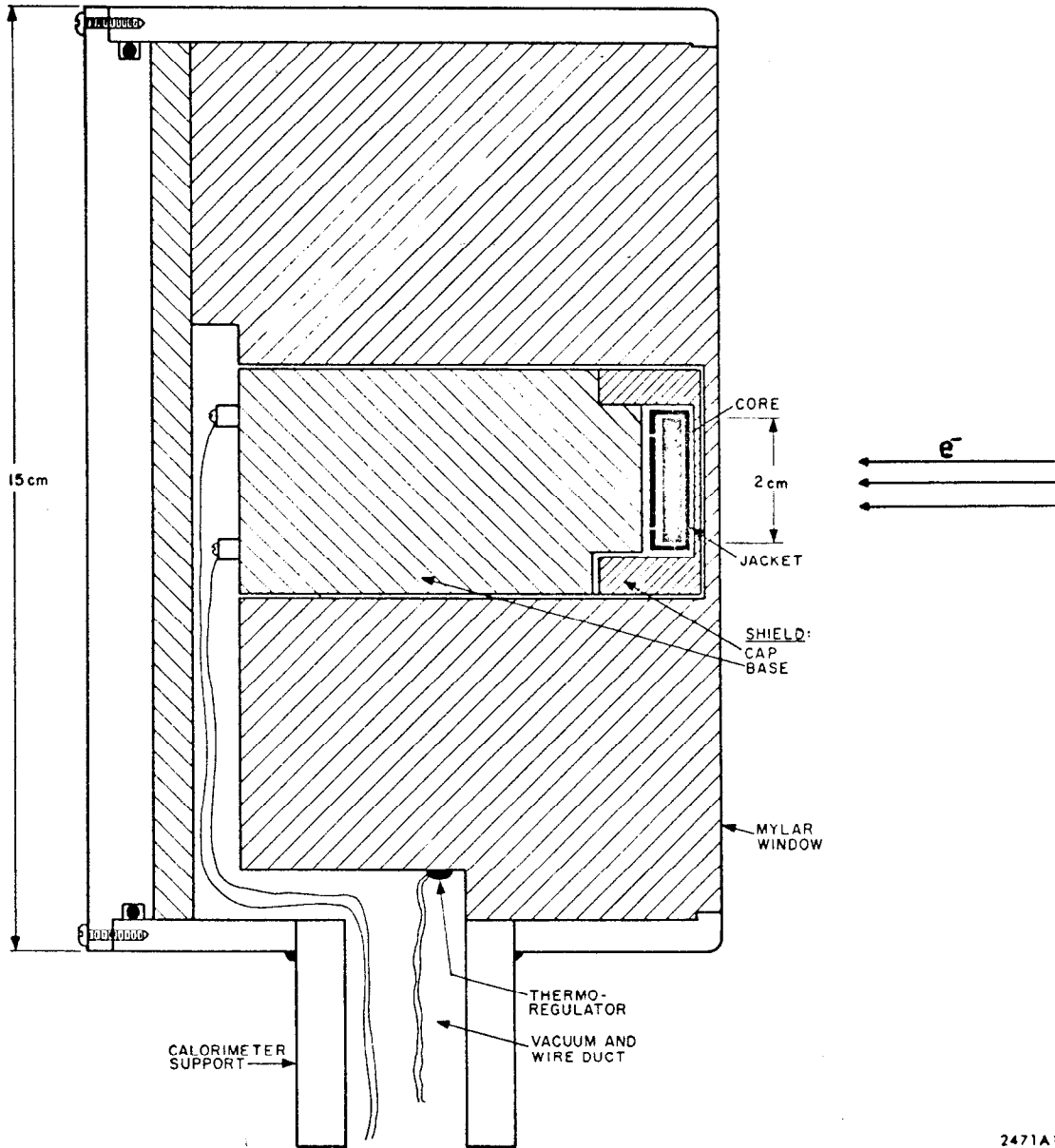


Fig. 1

2471A1

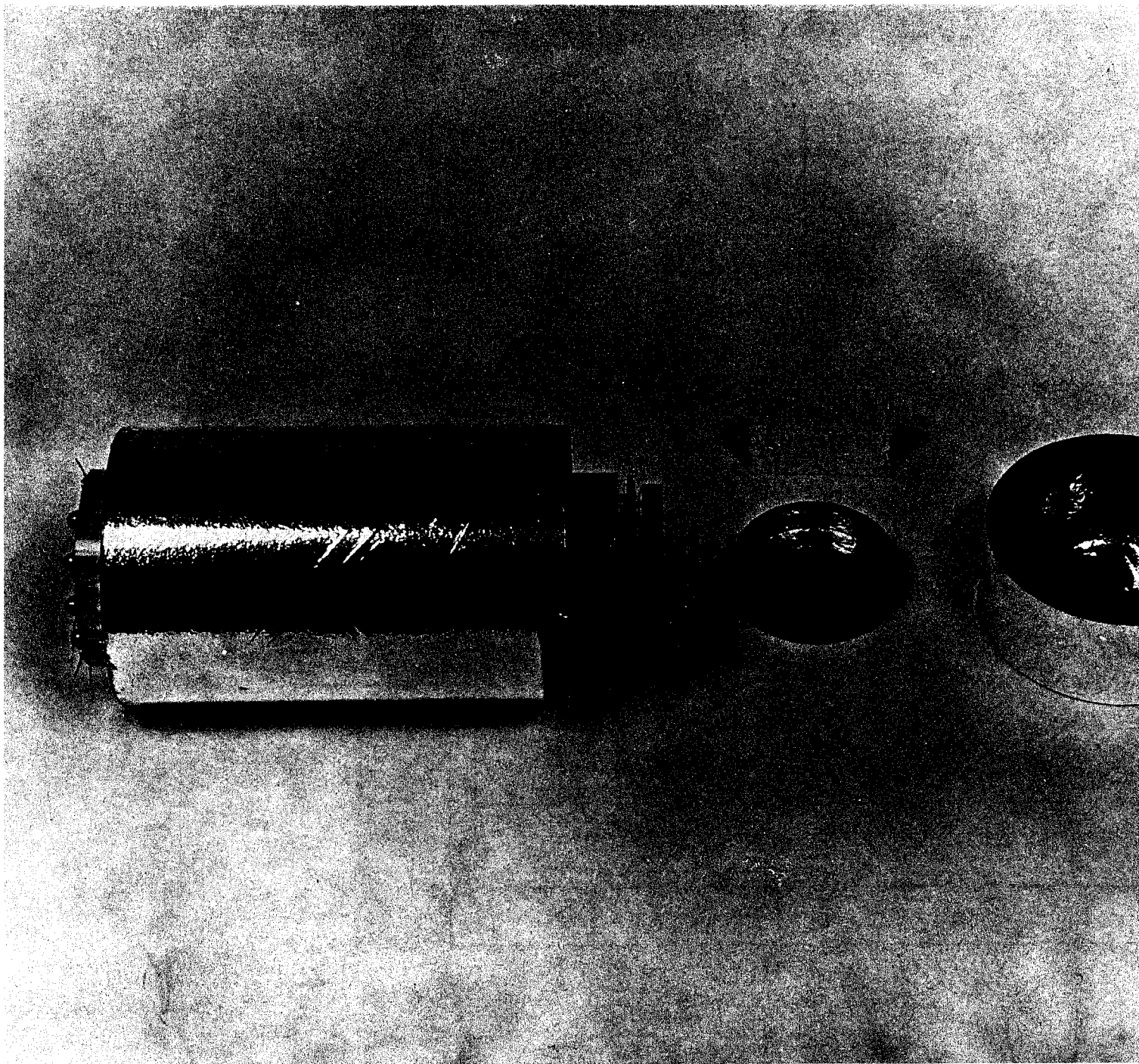


Fig. 2

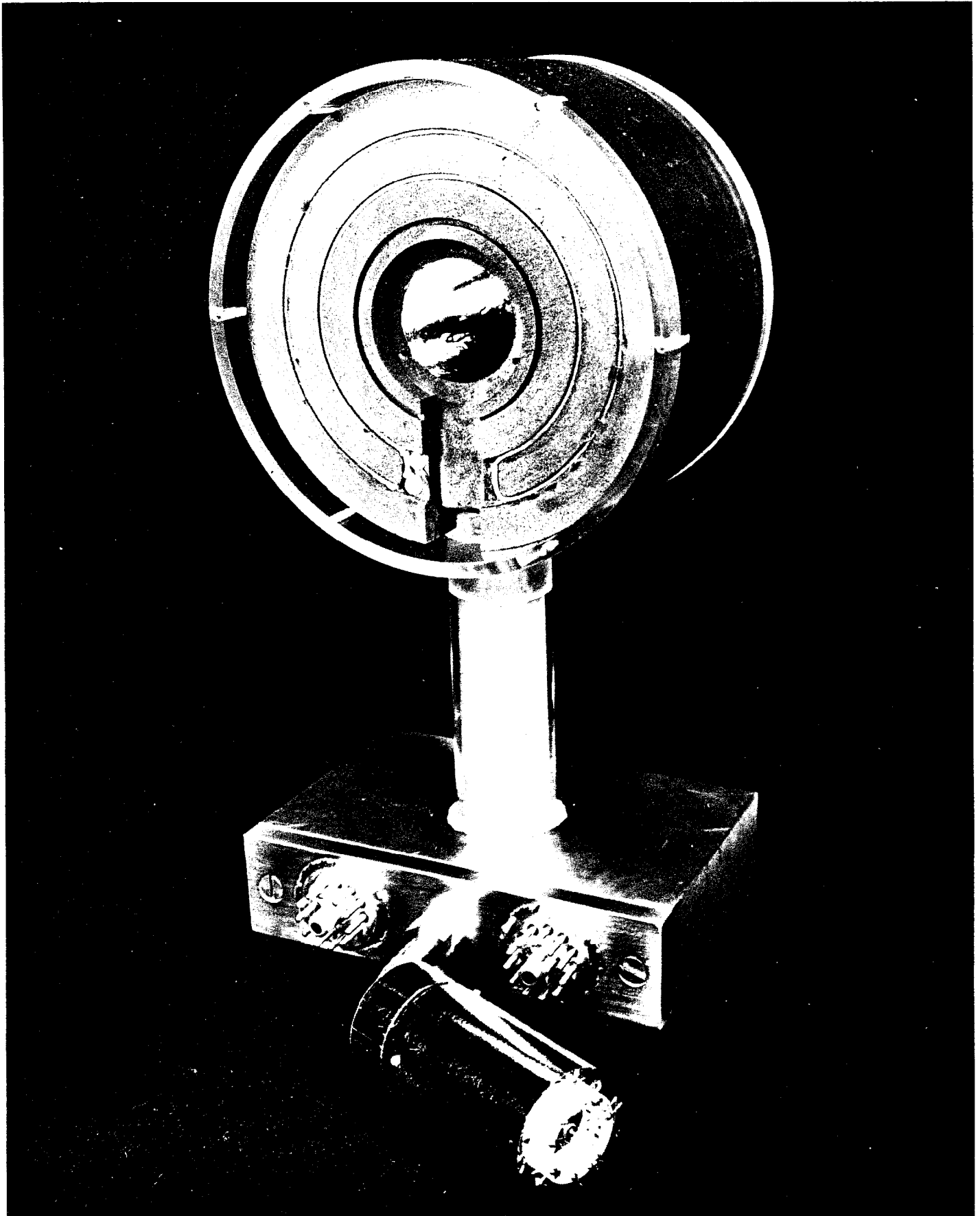


Fig. 3

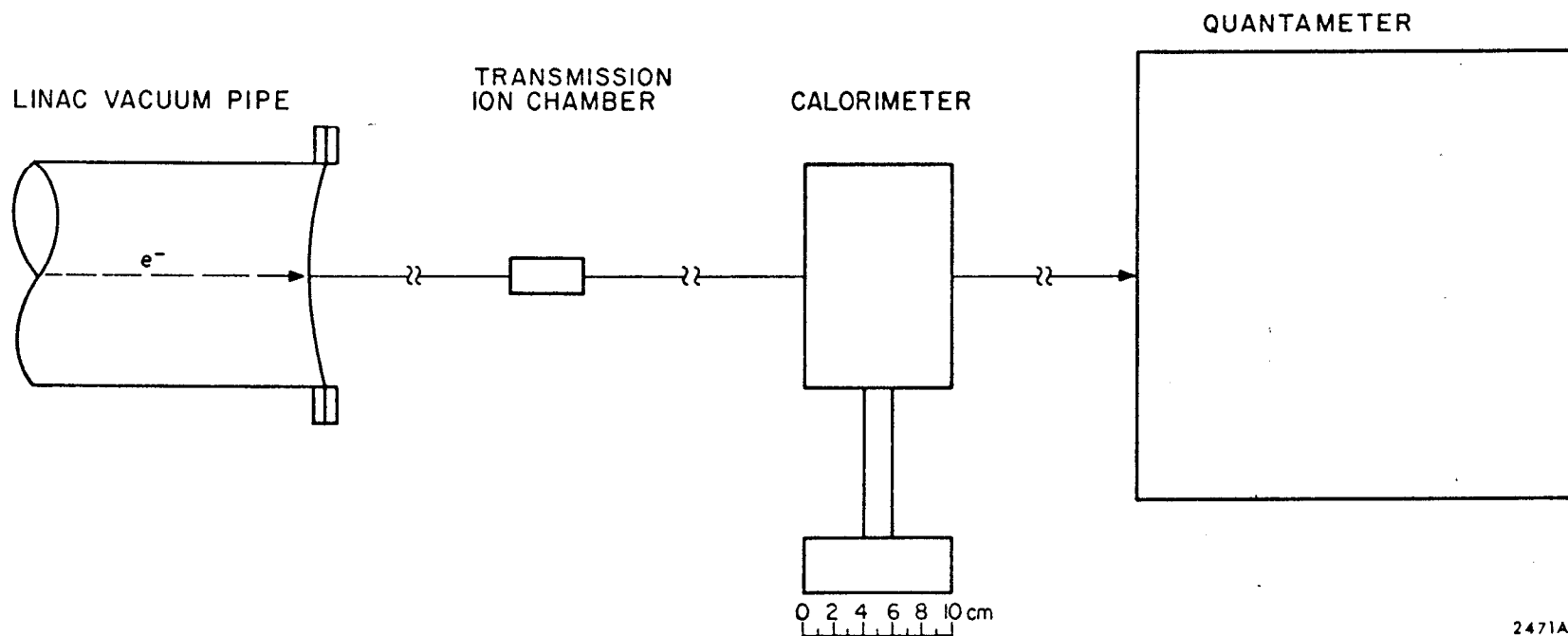


Fig. 4

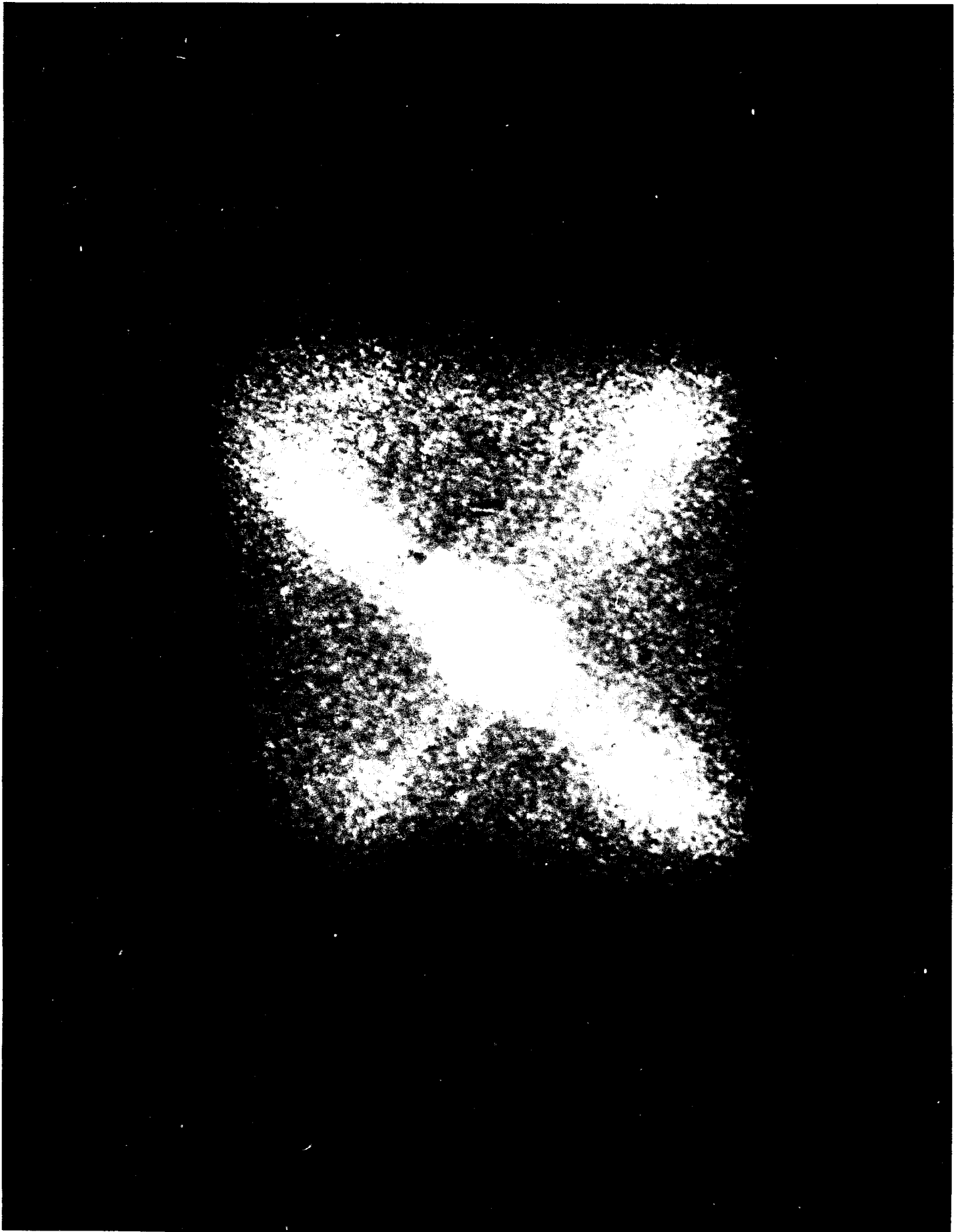


Fig. 5

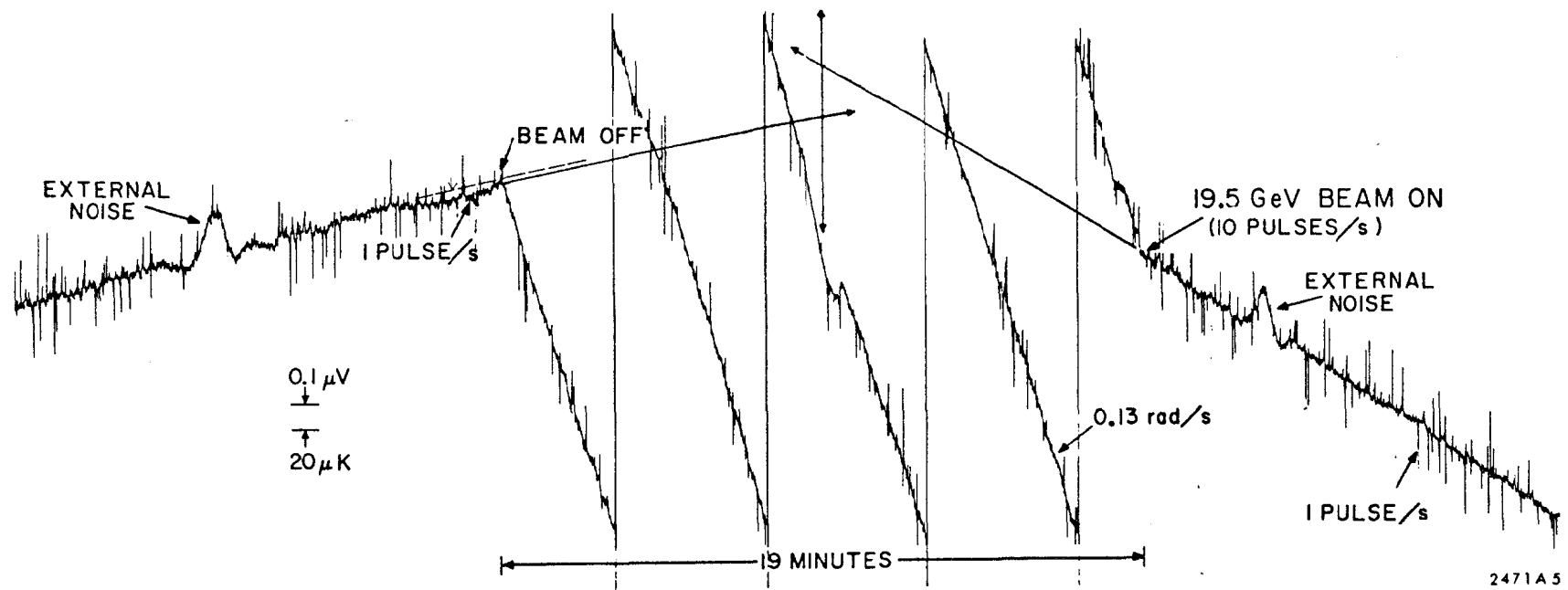
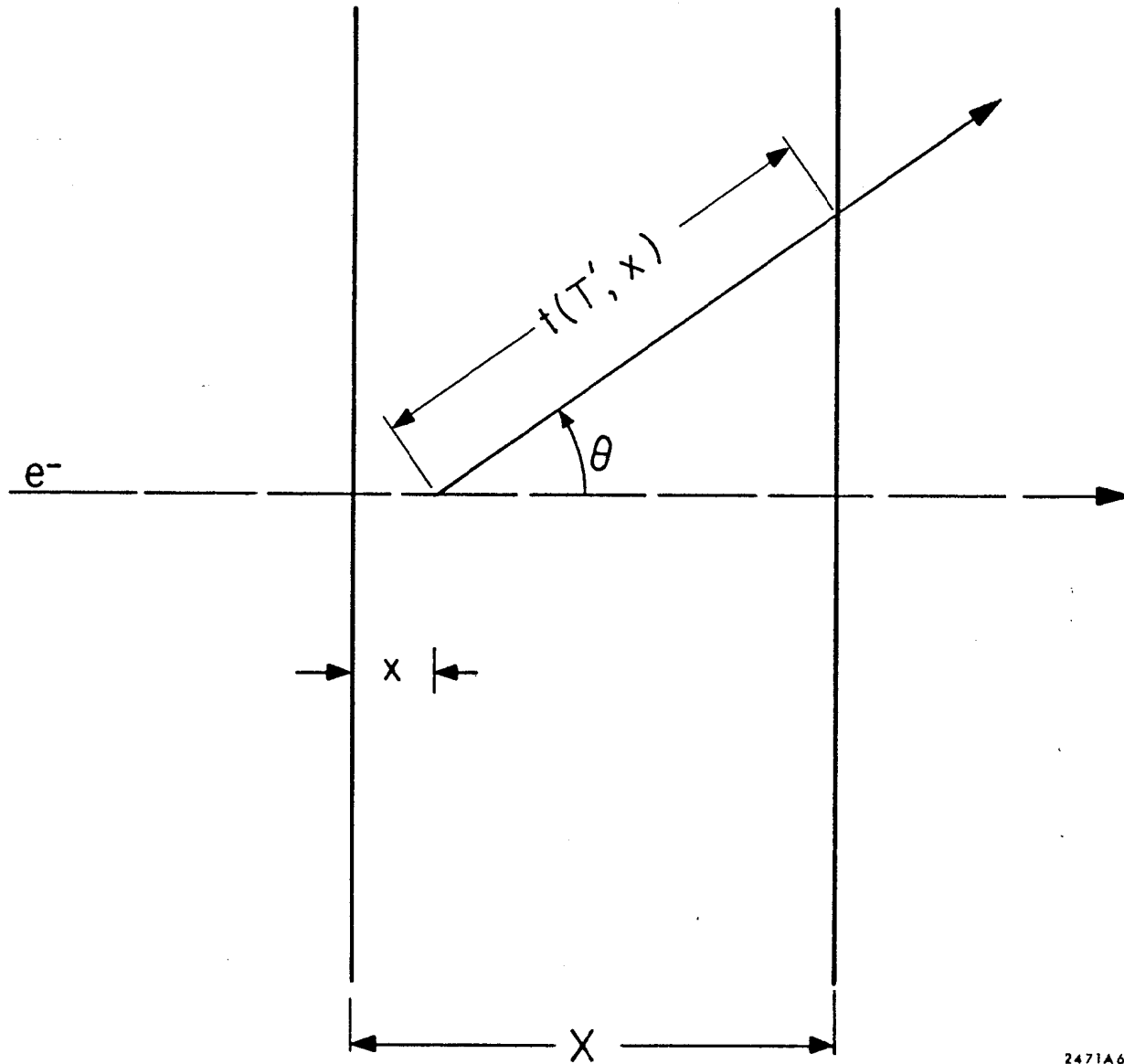
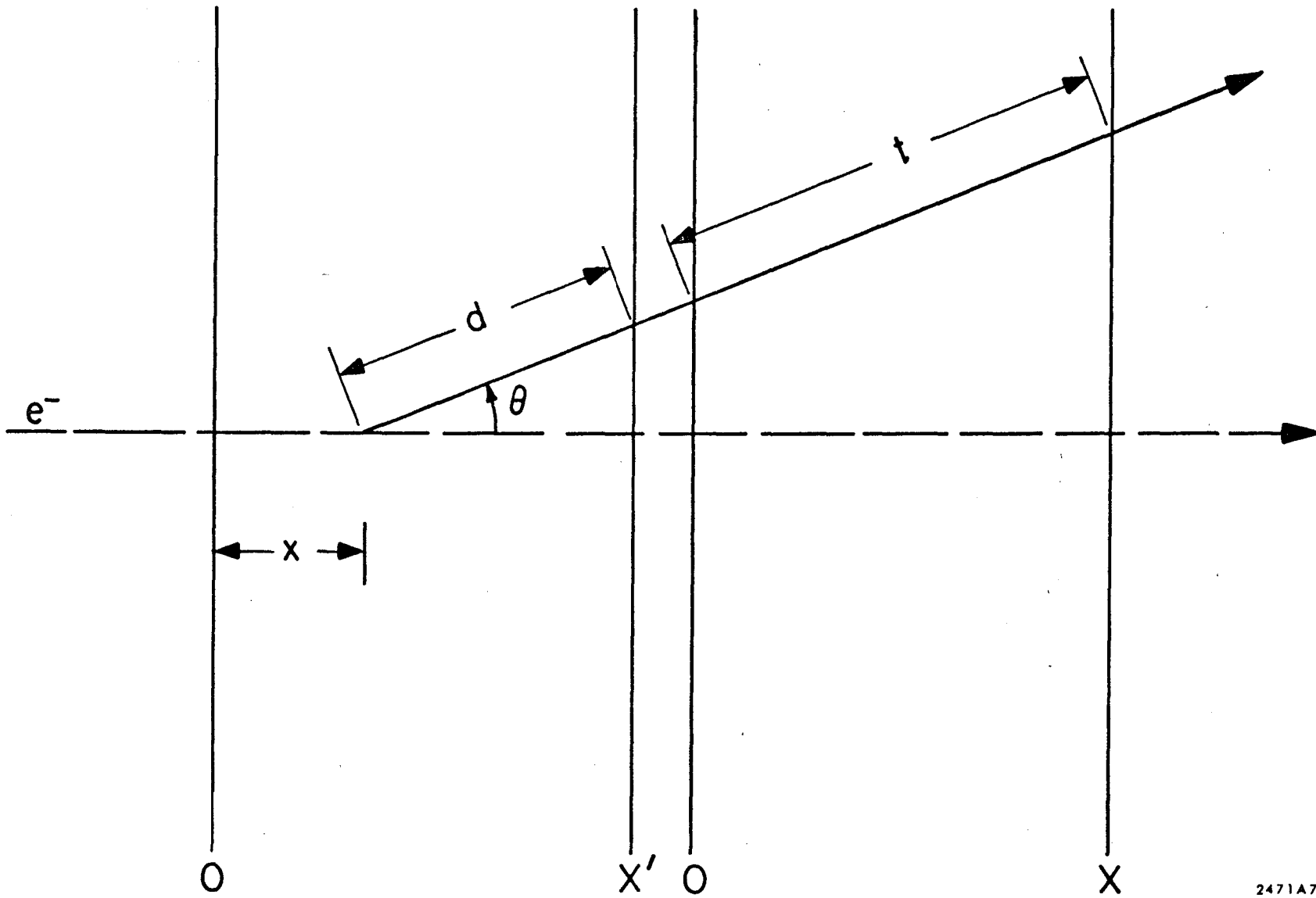


Fig. 6



2471A6

Fig. 7



2471A7

Fig. 8